Kinetics of solid phase interaction between Al and a-Si:H

Kinetics of solid phase interaction between Al and *a*-Si:H

Yuichi Masaki
Department of Electrical and Computer Engineering, Kanazawa University, Kodatsuno, Kanazawa 920, Japan

Toshihiro Ogata and Hiroshi Ogawa
Department of Electronic Engineering, Saga University, Honjyo, Saga 840, Japan

David I. Jones
Department of Applied Physics and Electronic and Manufacturing Engineering, University of Dundee, Dundee DD1 4HN, United Kingdom

The kinetics of solid phase interaction between Al and *a*-Si:H have been investigated. The experiment led to the observation of low-temperature crystallization as has been reported. The crystallization temperature was found to be 300–350 °C from diffraction studies. From the x-ray photoelectron spectroscopy study, electron transfer from Al to Si was observed in the intermixing layer in samples annealed at RT and 200 °C whereas there is no evidence of the electron transfer for 300 and 350 °C annealed samples. To explain these results, a comparison is made with the interaction in the Cr/*a*-Si:H system previously reported and the interdiffusion model is proposed.

I. INTRODUCTION

During the last few decades, aluminum (Al) has been one of the most successful electrode materials in Si integrated-circuit (IC) technology because of its low resistivity, good ohmic contact formation with Si, good adhesion to Si and SiO_2, and so on. The binary phase diagram of Al and Si shows the formation of the eutectic alloy at the temperature of 577 °C and a solid solution of Al with Si above 300 °C.[1,2] By utilizing the latter phenomenon, a sintering process is carried out in Si IC technology to make a good electrical contact between Al and Si at about 400–450 °C.

In *a*-Si:H device technology, on the other hand, the use of Al to make a direct contact with *a*-Si:H has been avoided, because Al atoms diffuse easily into *a*-Si:H and consequently the *a*-Si:H becomes metalliclike at an annealing temperature T_a as low as 200 °C.[3] Hence, Cr is often used as a diffusion barrier, being placed between Al and *a*-Si:H. It is also well known that the interaction between Al and *a*-Si(:H) induces the crystallization of the *a*-Si(:H) at a crystallization temperature T_c below 350 °C,[3–6] although the kinetics of such a low-temperature crystallization process have not been established.

Low-temperature Al-induced crystallization is consistent with the significant diffusion of Al atoms into the *a*-Si matrix where the Al atoms enhance an atomic rearrangement of the Si network by breaking Si—Si bonds.

It should be noted, on the contrary, that Al diffusion in *c*-Si is relatively slow. The diffusion kinetics of Al in *c*-Si have been ascribed to both the vacancy mechanism[7–9] and the interstitialcy mechanism.[8] In either case, an enthalpy for a vacancy formation is needed and consequently the diffusion coefficient is quite small compared with those of diffusants that follow a true interstitial mechanism such as transition metals or group-I and -VII elements.

In this article the kinetics of the low-temperature interaction at the interface between Al and *a*-Si:H is investigated and the various techniques employed are described. The results are then discussed and compared with those in the Cr/*a*-Si:H system described elsewhere.[10] Finally, the kinetic model of interdiffusion is proposed.

II. EXPERIMENTS

Undoped *a*-Si:H films were deposited onto a number of different types of substrate to a thickness of 800 Å by plasma-enhanced chemical-vapor deposition (PECVD). The deposition conditions of the films were same as those described in Ref. 10. The substrates used were oxidized Si wafers for infrared spectroscopy (IR), Corning 7059 glass for x-ray photoelectron spectroscopy (XPS) measurements, and carbon-coated mica films for transmission electron spectroscopy and diffraction (TEM and TED). After the deposition of *a*-Si:H films, Al films were thermally evaporated onto the surface of the *a*-Si:H films to a thickness of about 300 Å. Prior to the Al evaporation, native oxide on the *a*-Si:H films was removed by immersing the films into HF and by an Ar discharge. Samples for XPS and IR measurements were annealed in the temperature range of 200–350 °C for 30 min using a hot stage in a N_2 atmosphere. Subsequently for the samples used for the IR measurements, the residual Al layer at the top of the *a*-Si:H was chemically etched off. For electron-diffraction measurements, the Al/*a*-Si:H bilayer was floated off from the substrate by immersing the Al/*a*-Si:H/carbon-coated mica samples into pure de-ionized water, and the bilayer was spooned onto a stainless-steel mesh for the electron-diffraction experiments.

The electron-diffraction patterns were observed by TEM (JEOL STEM120), annealing the samples *in situ*. The annealing was carried out from RT to 350 °C with temperature steps of 50 °C and an annealing time of 30 min. The electron beam was incident on the samples only during the observation of the diffraction patterns in order to avoid any temperature rise due to the irradiation. A commercial XPS system (VG Scientific) using an Mg$K\alpha$ x-ray source with a resolution of 0.05 eV was used to measure photoemission spectra

Reprinted from J. Appl. Phys., Vol. 76, No. 9, pp. 5225(1994)

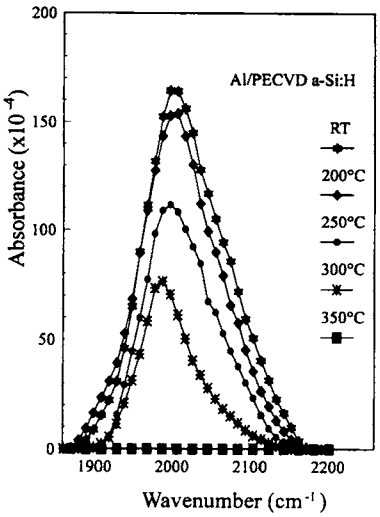

FIG. 1. IR absorbances in the wave-number range of 1850–2200 cm^{-1} for RT–350 °C annealed samples.

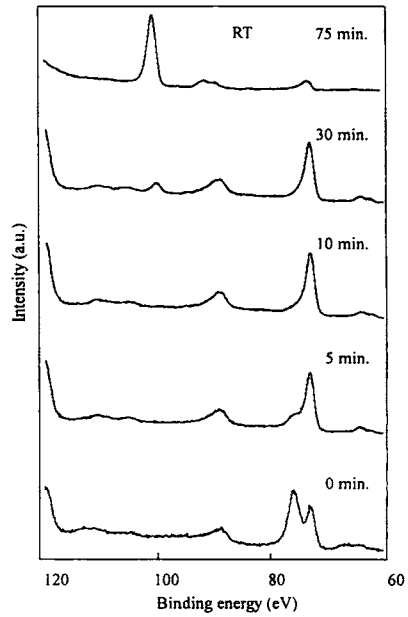

FIG. 2. Depth profiles of XPS spectra for RT sample.

(in the binding energy range 0–1100 eV) to different depths on samples annealed at RT, 200 °C, 300 °C, and 350 °C for 30 min. Sputtering was carried out *in situ* by Ar^+ for a sputtering time of 0–75 min to obtain the depth analysis.

III. RESULTS

A. Electron diffraction

The selected-area-diffraction (SAD) patterns for the samples annealed below 300 °C give a halo pattern representing *a*-Si:H, polycrystalline Al rings [Al(220), Al(311), and so on], and polycrystalline C (graphite structure) rings [C(220), C(110), and so on]. The appearance of C rings is due to the contamination from the carbon-coated mica substrate. On the other hand, the SAD pattern for the 350 °C anneal sample shows polycrystalline Si (poly-Si) rings [Si(111), Si(220), Si(311), and so on] and also polycrystalline C rings. The corresponding TEM image reveals that the growth of poly-Si was dendritelike. Hence, we can say that the crystallization of *a*-Si:H takes place at a temperature between 300 and 350 °C as was previously reported.[3,4]

B. IR

IR absorbances in the wave-number range of 1850–2200 cm^{-1}, which corresponds to Si-H_x stretching modes, are shown in Fig. 1 for different annealing temperatures. In the figure, two absorbances can be observed around 2000 and around 2080 cm^{-1}. The former absorbance is associated with the Si-H stretching vibration and the latter with the H-Si-H stretching mode.[11] As shown in the figure, for the sample annealed at T_a=200 °C the absorbance is not significantly different from the unannealed sample. Above T_a=250 °C, however, with increasing T_a the absorbance decreases and at T_a=350 °C (when *a*-Si:H was already crystallized) it becomes negligible. This probably indicates that the amount of hydrogen in the film becomes insignificant while the amount of H remaining in *a*-Si:H without any metal contact is not negligible at such a low annealing temperature. This tendency is very similar to what was observed in the Cr/*a*-Si:H system where the amount of H becomes negligibly small when *c*-Cr silicides are formed as has been described in Ref. 10.

C. XPS

Figure 2 shows the XPS spectra in the binding-energy range of 60–120 eV for nonannealed samples obtained after etch (sputtering) times of 0, 5, 10, 30, and 75 min. In the diagram, before etching peaks due to Al(metal)2*p*, Al(oxide)2*p*, Al 2*p* plasmon, Al(metal)2*s*, and Al(oxide)2*s* photoelectrons are observed at the binding energies of about 73, 76, 88, 118, and 120 eV, respectively. After etching the same samples for 75 min the peaks due to Al(oxide) disappear and that due to Si(metal)2*p* photoelectrons around 99 eV appears.

Atomic compositional ratios of Si, Al, and O determined from the areas under the Si(metal+oxide)2*p*, Al(metal +oxide)2*p*, and O 1*s* (appearing around 532 eV) peaks are shown as a function of etch time in Figs. 3(a)–3(d) for the RT, 200 °C, 300 °C, and 350 °C anneal samples, respectively. Since the sputtering yield for Al by Ar^+ is twice as high as that for Si,[12] i.e., 1.05 for Al compared with 0.50 for Si, the etch times indicated on the horizontal axis in the diagrams do not correspond to the real etch depth. Figure 3 shows clearly that by annealing above 300 °C Si atoms out-

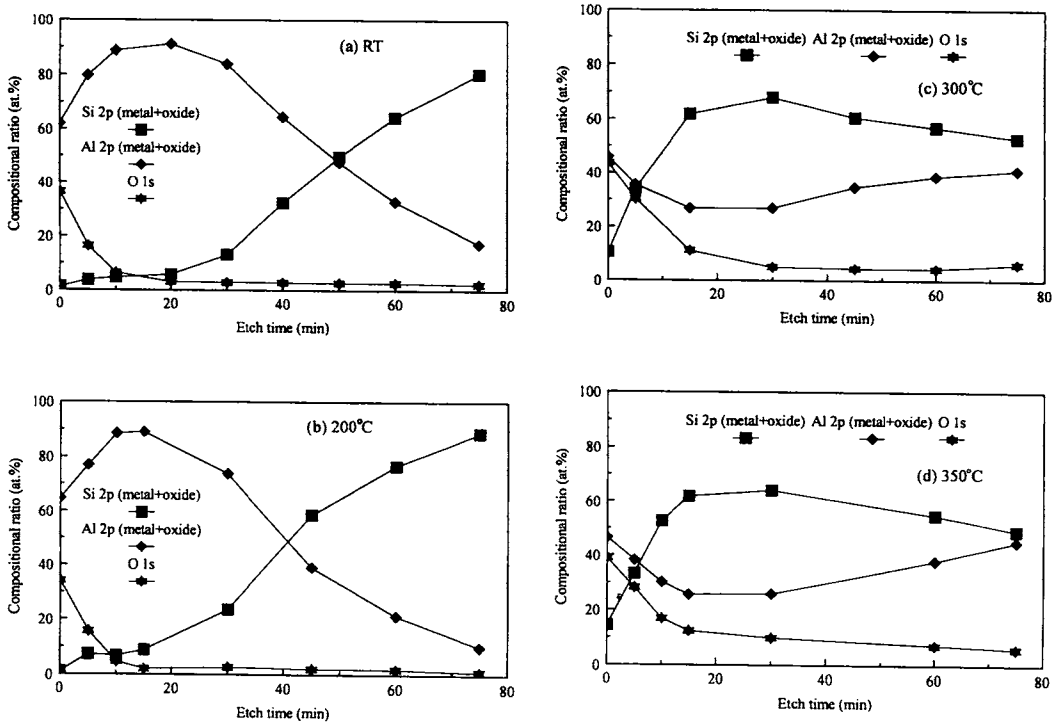

FIG. 3. Atomic compositional ratios of Si, Al, and O for (a) RT, (b) 200 °C annealed, (c) 300 °C annealed, and (d) 350 °C annealed samples.

diffuse toward the surface of the film and Al atoms indiffuse and move further into the a-Si:H. It should be noted that even at RT interdiffusion between Al and Si takes place and Si atoms tend to outdiffuse to the film surface.

Figures 4(a)–4(d) show the binding energy (BE) as a function of etch time for Si(metal)$2p$(3/2) and Al(metal)$2p$(3/2) photoelectrons for RT, 200 °C, 300 °C, and 350 °C anneal samples, respectively. For RT and 200 °C anneal samples, the BEs for both Si and Al increase with increasing depth, but remain nearly constant for samples annealed at 300 and 350 °C, i.e., about 99.15 eV for the Si $2p$, and about 72.7 eV for the Al $2p$, respectively. Although the BEs for pure Si and pure Al were not measured in this system, these energies can be estimated from Figs. 4(a) and 4(b) because the interaction between Al and a-Si:H is still weak at T_a<200 °C as shown in Fig. 3. At the surface, it may be assumed that the BE of pure Al is measured. This value at zero etch time is 72.7 eV. At maximum etch time where there is little Al concentration, the BE of pure Si is seen to be 99.2 eV. By considering the interaction region at which atomic concentrations of Al and Si are nearly same in samples annealed at RT and 200 °C [see Figs. 3(a) and 3(b)], for example, an etch time of 50 min for the RT sample or an etch time of 40 min for the 200 °C sample, it is obvious that the BE for the Si $2p$ is smaller than that for pure Si and that of the Al $2p$ is larger than that for pure Al. We therefore conclude that electron transfer takes place from Al to Si, maybe due to the difference in electronegativities (1.61 for Al and 1.90 for Si), so that the Al atom makes a weak bond with Si. On the other hand, for the 300 and 350 °C anneal samples, it is found that the BEs for Si $2p$ and Al $2p$ take the values of that for pure Si and pure Al, respectively, independent of both the etch time and the atomic ratio.

IV. DISCUSSION

The experimental results previously reported[10,13] indicate that prior to crystallization internal energy in the a phase is released by (1) hydrogen evolution, (2) intermixing of a metal and Si, and (3) a structural change in the a-Si network itself. This release of internal energy results in bonding states in the a phase becoming like those in the c phase. In this section we discuss why such structural change takes place at the comparatively low temperature of 300–350 °C when Al is in contact with a-Si:H and consider in detail the intermixing mechanism.

We first consider the initial change in the interface structure between Al and a-Si:H and compare it with that in the Cr/a-Si:H case.[10] Miedema, Châtel, and de Boer's method[14] for calculating the heat of a-Cr silicide formation indicates that the silicide is more stable than both Cr and a-Si:H. A similar calculation for the Al/a-Si:H system gives an exothermic heat of reaction of 10.1 kJ/mol for the formation of a-Al_5Si_{95}. This indicates that the a-AlSi alloy is also ener-

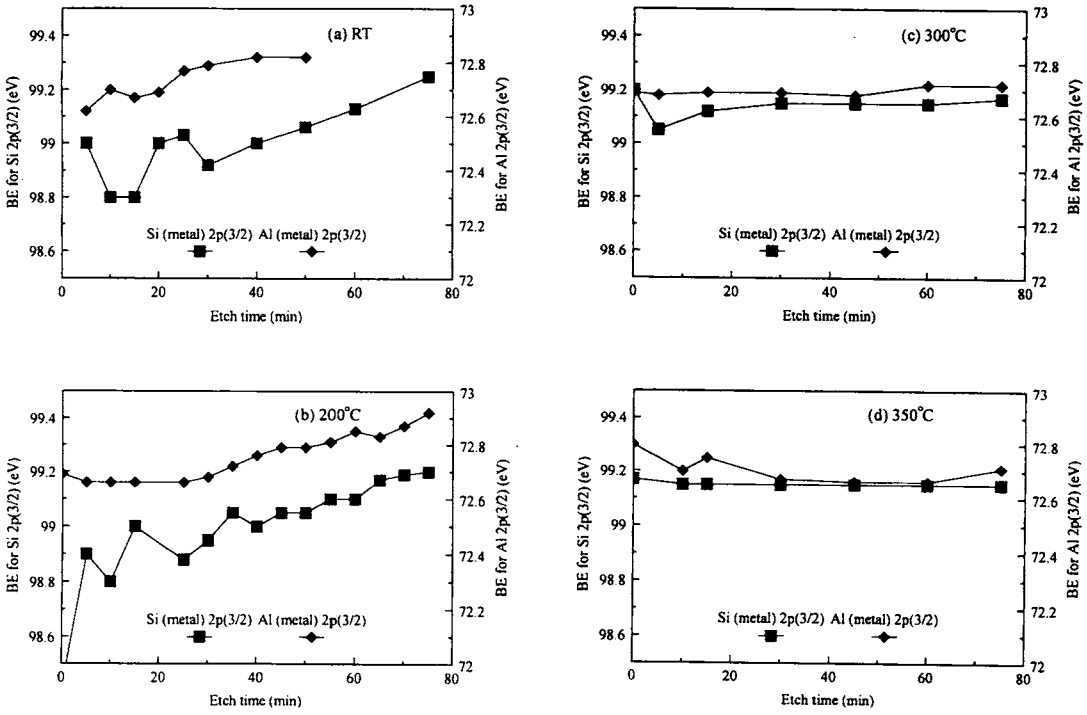

FIG. 4. Binding energies for Si (metal) $2p(3/2)$ and Al(metal) $2p(3/2)$ photoelectrons for (a) RT, (b) 200 °C annealed, (c) 300 °C annealed, and (d) 350 °C annealed samples.

getically more stable than both Al and *a*-Si:H. It is therefore valid to apply the model[10] proposed for the Cr/*a*-Si:H system to the present Al/*a*-Si:H system. In the model[10] it was proposed that the intermixing in the contact layer must continue until the interfacial electric field [which is created at the interface between a metal and *a*-Si:H due to the difference in their electronegativities as shown in Fig. 5(a)] becomes negligibly small. Figure 5(b) illustrates the band diagram for the Cr/*a*-Si:H system after the initial intermixing where the internal field is negligible. It was also assumed that the intermixing in the Cr/*a*-Si:H system took place mainly by interdiffusion of ionized atoms.[10]

For the Al/*a*-Si:H system, we can conclude that at RT a stronger interaction exists between Al and *a*-Si:H compared with that in the Cr/*a*-Si:H system because the difference in the electronegativity between Al and Si is larger than that between Cr and Si. In addition, in contrast to the Cr/*a*-Si:H system in which electron transfer between Cr and Si is not observed, for the RT and 200 °C anneal samples, electron transfer is seen between Al and Si in the regions of intermixing, which means that the intermixing process is not complete. Figure 5(c) shows the band diagram for the Al/*a*-Si:H case after the initial intermixing. In the same way as *a*-Cr silicide formation,[10] an internal field created by the Al/*a*-Si:H contact [see Fig. 5(a)] must be compensated, in other words the Fermi energy E_F must be coincident throughout the system. To compensate the field, ionized atoms which are caused by the electron transfer interdiffuse at the Al/*a*-Si:H interface and consequently intermixing takes place. The experimental results shown in Figs. 3 and 4 also support that the compensation for the field is made by atomic diffusion rather than electron diffusion. In Fig. 5(c), however, an internal field between Al and *a*-Si:H is still present and the reason for this is explained below. Also, some fraction of the Al atoms goes into substitutional sites as acceptors in the Si matrix because *p*-type characteristics have been observed in *a*-AlSi:H alloy even with 0.5 at. % Al,[15] and this is taken into account in the diagram.

From the above argument it is clear that the only significant difference between the Al/*a*-Si:H and the Cr/*a*-Si:H systems during the initial change in the interface structure is that electron transfer takes place in the intermixing region in the former system. Therefore, second, we consider why the electron transfer is observed in the present system while it is not seen in the Cr/*a*-Si:H system.[10] The most plausible reason is that in the Cr/*a*-Si:H system the interaction ceases or becomes negligible within a shallow region whereas in the Al/*a*-Si:H system it is still continuing because in a low temperature anneal, e.g., 300 °C, a considerable number of Al atoms diffuses to a greater depth in the *a*-Si:H as shown in Fig. 3(c) while the *a*-Cr silicide is rather thin.[10]

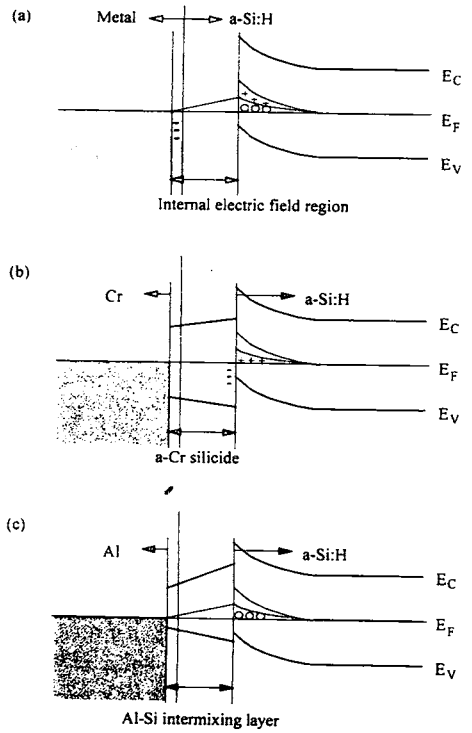

FIG. 5. Band diagrams for (a) the initial state of a metal/a-Si:H contact and states after intermixing for (b) the Cr/a-Si:H and (c) the Al/a-Si:H systems. + and − represent positively charged and negatively charged states, respectively, and ○ represents an electron.

Third, we consider why the Al/a-Si:H system is much more reactive than the Cr/a-Si:H system from the viewpoint of the kinetics of diffusion and make an assumption of a self-sustaining intermixing model for the present system. Figure 6 shows a schematic illustration of a metal/a-Si:H system with an appropriate depth profile of the atomic concentrations for the metal and Si after initial intermixing [for example, the Cr/a-Si:H system shown in Fig. 5(b) where the internal field is negligible]. In Fig. 6, the arrows show the directions of the atomic fluxes when the interdiffusion takes place. If it is assumed that it is possible for the compositional equilibrium shown in Fig. 6 to be disturbed a little by interdiffusion of the metal and Si, e.g., excess Si atoms appear at the metal/alloy interface and excess metal atoms at the alloy/a-Si:H interface, a new field is induced. Consequently the intermixing between metal and Si is restarted by the new field and continues until the field becomes negligible again. This is the key process in the self-sustaining intermixing model assuming for the present Al/a-Si:H system. Figure 7(b) summarizes in the form of a flow chart the mechanism for the a-AlSi alloy formation compared with that for the a-Cr silicide formation [Fig. 7(a)]. In the flow chart, a process [A] shows a metal/a-Si:H contact before reaction; at [B] the contact induces an internal field because of the difference

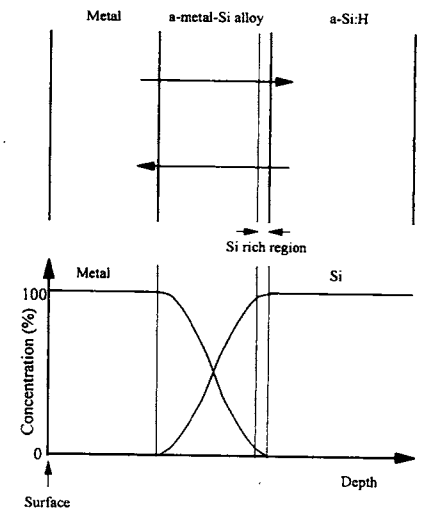

FIG. 6. Schematic illustration of a metal/a-Si:H system with a corresponding depth profile of the atomic concentrations for the metal and Si where the internal field is negligible. Once this compositional equilibrium is disturbed, however, a new field arises.

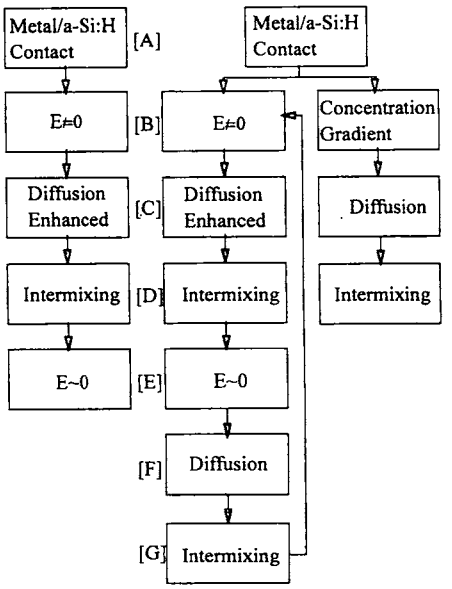

(a) Cr/a-Si:H system (b) Al/a-Si:H system

FIG. 7. Flow charts of the intermixing mechanism for (a) the Cr/a-Si:H system and (b) the Al/a-Si:H system. For the Cr/a-Si:H system the intermixing process terminates at process [E] whereas for the Al/a-Si:H system the self-sustaining process and a general diffusion mechanism coexist.

in their electronegativities; at [C] the internal field enhances the interdiffusion of the metal and Si atoms; at [D], consequently, the intermixing layer is created; and at [E], after the intermixing, the internal field becomes negligibly small. For the Cr/*a*-Si:H system, the intermixing process terminates here, but for the Al/*a*-Si:H system a process [F], interdiffusion without internal field, takes place and the region of intermixing grows [G] which is the situation described in [B]. As shown in the flow chart (b), for the Al/*a*-Si:H system the intermixing would continue cyclically until the Al and Si atoms mix entirely with each other. It should be noted that the intermixing indicated by process [G] is less reactive than that by process [D].

We now have to discuss further whether the process [F] in the flow chart, i.e., interdiffusion without field at a low temperature, is possible. The atomic diffusion phenomena in the intermixing AlSi (alloy) region must therefore be considered. As far as is known, information on diffusion phenomena is available only for diffusion in Si-rich regions of an alloy which is not dissimilar to *a*-Si:H with a high impurity concentration and therefore the information is of relevance in this discussion.

The Si solid phase crystallization (SPC) experiments provide some insight to the Si diffusion in such a Si-rich region. Bisaro *et al.*[16] have studied the kinetics of the Si SPC with respect to the doping concentration in *a*-Si and observed that the growth velocity of *c*-Si increases with increasing doping concentration and is independent of the type of dopant. They found that the growth velocity increased by a factor of 6 for boron (B) doping when $B_2H_6/SiH_4=2\times10^{-3}$ and they quoted the results of Csepregi *et al.*[17] which showed that the enhancement of the growth velocity was about 25 when the B concentration was 2.5×10^{20} cm^{-3}. The Si self-diffusion in the *a*-Si matrix is closely associated with the growth velocity and is independent of the type of dopant. This contrasts with the Si self-diffusion in the *c*-Si matrix in which the self-diffusivity is enhanced by an *n*-type doping, but is retarded by a *p*-type doping.[18] This implies that the mechanism of self-diffusion in *a*-Si is different from that in *c*-Si. From these experimental results and electron-spin-resonance (ESR) results, Bisaro *et al.* found a clear correlation between the increase in the growth velocity and the decrease in the concentration of neutral dangling bonds, and concluded that the growth of *c*-Si (or the Si self-diffusion in *a*-Si) was associated with the charged dangling bonds rather than the vacancies which were considered to be the main influence in the self-diffusion in *c*-Si.

Diffusion data for dopant impurities in *a*-Si:H are also available. Matsumura, Maeda, and Furukawa[19,20] have measured the diffusion coefficients of B and Sb in PECVD *a*-Si:H, which are obtained from impurity profiles determined by the Rutherford backscattering (RBS) technique. They reported that the temperature dependence of the diffusion coefficient of B was almost the same as that of Sb and not very different from what had been previously measured for hydrogen. From this observation and the results of both conductivity measurements and the H content dependence of the diffusion coefficients, they concluded that (1) such dopant impurities diffused following the movement of H and (2) the electrically active impurities, i.e., substitutional dopants, diffused easier than inactive impurities.

The H diffusion in *a*-Si:H must now be considered. According to the Street,[21] H diffusion is strongly dependent on the doping concentration. In particular, in B-doped *a*-Si:H with a concentration of 10^{-2} B, the diffusion coefficient is enhanced by a factor of 10^3 with respect to that in undoped *a*-Si:H. In addition the study of diffusion in a compensated *a*-Si:H suggests that this doping related effect is electronic rather than structural in origin.

There is less information on the diffusion process of interstitial diffusants such as Cr; however, it is possible to obtain some understanding of interstitial diffusion from the work reported by Beyer, Herion, and Zastrow.[22] They have studied the diffusion of Li in *a*-Si:H for different doping concentrations and found that the process was greatly enhanced by the B doping, in particular, the enhancement was found to be more than 10^3 by adding a few % B_2H_6/SiH_4 in the deposition gas phase.

The experimental evidence suggests that in the presence of dopant atoms the diffusion coefficients of hydrogen, Si, and impurity atoms (including both dopant and nondopant atoms) can be considerably enhanced. In addition, in the present system where a Si concentration gradient exists, the Si self-diffusion coefficient could be much larger compared with the case where there is no concentration gradient, as has been shown by the Si SPC experiments.

To explain the above behavior, the following tentative model is finally proposed for the Al/*a*-Si:H system. From the arguments given above, a self-sustaining model may be applied for the Al/*a*-Si:H system; however, a survey of atomic diffusion phenomena indicates that even without an internal field diffusivity of H, Si, and Al atoms is significant. Hence, it may be reasonable to consider that a self-sustaining interdiffusion mechanism and a general diffusion mechanism due to a concentration gradient coexist. Experimentally they are difficult to separate because diffusion due to these two mechanisms is proportional to the inverse of the distance for both.

It can be concluded that the Al atoms are in both substitutional and interstitial sites in the *a*-Si:H matrix while the Cr atoms do not go into the substitutional sites. The substitutional Al atoms behave as acceptors in *a*-Si:H and consequently could contribute the enhancement of the diffusion of Al, Si, and H atoms. Hence, an internal field in the *a*-AlSi alloy is continuously created. As a result, the XPS results showed the electron transfer between Al and Si. On the other hand, in the Cr/*a*-Si:H system, such a dopant-related effect never takes place and consequently clear evidence was not observed of an interdiffusion after an initial *a*-silicide formation as shown in Ref. 10.

Metals which give rise to an alloy with Si even at room temperature are those which diffuse more readily into the *a*-Si matrix. In terms of the model proposed here, this implies that they are more efficient at breaking bonds and inducing rearrangement of the Si network. To achieve metal-induced low-temperature crystallization of *a*-Si(:H) for technological purposes, it is therefore concluded that metals capable of substitutional insertion into Si be employed. In

addition, as large a difference as possible in electronegativity between the metal and the silicon should be preferable.

V. CONCLUSIONS

In order to gain some insight on the kinetics of interdiffusion between Al and *a*-Si:H, the XPS study has mainly be carried out. The following summarize the main experimental results.

(1) The presence of Al in contact with *a*-Si:H induced the crystallization of *a*-Si:H at the temperature range of 300–350 °C as has been reported, which is much lower than the crystallization temperature of *a*-Si:H without contact to Al.
(2) For the RT and 200 °C annealed samples, the electron transfer from Al to Si was observed in the regions where intermixing took place. On the other hand, for the 300 and 350 °C annealed samples, there was no evidence of such an electron transfer.

By comparing these results with those obtained in the investigation of interaction between Cr and *a*-Si:H, an intermixing model involving a self-sustaining and a general diffusion mechanism has been proposed.

Thus, metal atoms which go into substitutional sites in an *a*-Si:H matrix enhance diffusion of the metal, Si, and H, and therefore an internal field is continuously created. As a result, the intermixing continues until the metal and Si atoms mix entirely with each other. On the other hand, for a system in which such a dopant effect does not take place, intermixing between metal and Si atoms ceases after initial intermixing.

ACKNOWLEDGMENTS

The authors are deeply grateful to Dr. J. Robertson of the National Power Research Laboratory for fruitful discussions. Thanks also go to Professor A. G. Fitzgerald, Dr. R. A. G. Gibson, and Dr. M. J. Rose of Dundee University for their help and many discussions during this work. Special thanks are also due to S. Anthony and K. Duncan for preparing and measuring samples.

[1] W. G. Moffatt, *The Handbook of Binary Phase Diagrams* (Genium, New York, 1987).
[2] R. M. Hansen, *Constitution of Binary Alloy*, Metallurgy and Metallurgical Engineering Series (McGraw-Hill, New York, 1958).
[3] S. Ishihara, M. Kitagawa, and T. Hirao, J. Appl. Phys. **62**, 837 (1987).
[4] S. R. Herd, P. Chaudhari, and M. H. Brodsky, J. Non-Cryst. Solids **7**, 309 (1972).
[5] G. Radnoczi, A. Robertson, H. T. G. Hentzell, S. F. Gong, and M.-A. Hasan, J. Appl. Phys. **69**, 6394 (1991).
[6] T. J. Konno and R. Sinclair, Philos. Mag. B **66**, 749 (1992).
[7] R. B. Fair, in *Semiconductor Materials and Process Technology Handbook for VLSI and ULSI*, edited by G. E. McGuire (Noyes Publications, Park Ridge, NJ, 1988).
[8] B. L. Sharma, Defect and Diffusion Forum **70&71**, 1 (1990).
[9] J. C. C. Tsai, in *VLSI Technology*, edited by S. M. Sze (McGraw-Hill, New York, 1983).
[10] Y. Masaki, S. Nonomura, R. A. G. Gibson, T. Sakimoto, T. Kurokawa, and H. Kawai, J. Non-Cryst. Solids **164-166**, 857 (1993).
[11] K. Morigaki, E. Maruyama, T. Shimizu, F. Yonezawa, M. Hirose, and K. Tanaka, in *Amorufasu Handotai no Kiso* (Fundamentals of Amorphous Semiconductors), edited by M. Kikuchi (Ohm-sha Ltd., Tokyo, 1982) (in Japanese).
[12] J. L. Vossen and J. J. Cuomo, in *Thin Film Processes*, edited by J. L. Vossen and W. Kern (Academic, New York, 1987).
[13] Y. Masaki, P. G. LeComber, and A. G. Fitzgerald, J. Appl. Phys. **74**, 129 (1993).
[14] A. R. Miedema, P. F. de Châtel, and F. R. de Boer, Physica B **100**, 1 (1980).
[15] J. L. Andújar, J. Andreu, G. Sardin, J. C. Delgado, J. Esteve, and J. L. Morenza, Solid Energy Mater. **15**, 167 (1987).
[16] R. Bisaro, J. Magariño, K. Zellama, S. Squelard, P. Germain, and J. F. Morhange, Phys. Rev. B **31**, 3568 (1985).
[17] L. Csepregi, E. F. Kennedy, T. J. Gallagher, J. W. Mayer, and T. W. Sigmon, J. Appl. Phys. **48**, 4234 (1977).
[18] S. M. Hu, in *Atomic Diffusion in Semiconductors*, edited by D. Shaw (Plenum, London, 1973).
[19] H. Matsumura, M. Maeda, and S. Furukawa, Jpn. J. Appl. Phys. **22**, 771 (1983).
[20] H. Matsumura, M. Maeda, and S. Furukawa, J. Non-Cryst. Solids **59&60**, 517 (1983).
[21] R. A. Street, *Hydrogenated Amorphous Silicon* (Cambridge University Press, Cambridge, 1991).
[22] W. Beyer, J. Herion, and V. Zastrow, J. Non-Cryst. Solids **137&138**, 111 (1991).